Decline in Atlantic Primary Production Accelerated by Greenland Ice Sheet Melt

Lester Kwiatkowski, Joseph Naar, Laurent Bopp, Olivier Aumont, Dimitri Defrance, Damien Couespel

Geophysical Research Letters

RESEARCH LETTER
10.1029/2019GL085267

Decline in Atlantic Primary Production Accelerated by Greenland Ice Sheet Melt

Lester Kwiatkowski[1], Joseph Naar[1], Laurent Bopp[1], Olivier Aumont[2], Dimitri Defrance[3], and Damien Couespel[2]

[1]Laboratoire de Météorologie Dynamique (LMD), IPSL, CNRS, Ecole Normale Supérieure/PSL Res. Univ., Ecole Polytechnique, Sorbonne Université, Paris, France, [2]Laboratoire d'Océanographie et de Climatologie: Expérimentation et Approches Numériques (LOCEAN), IPSL, CNRS, Sorbonne Université, IRD, MNHN, Paris, France, [3]SYSTEM, Univ Montpellier, INRA, Montpellier SupAgro, CIRAD, CIHEAM, Montpellier, France

Abstract Projections of climate impacts on marine net primary production (NPP) are reliant on Earth System Models (ESMs) that do not contain dynamic ice sheets. We assess the impact of potential Greenland ice sheet meltwater on projections of 21st century NPP using idealized ESM simulations. Under an extreme melt scenario, corresponding to 21st century sea level rise close to 2 m, Greenland meltwater amplified the decline in global NPP from a decrease of 3.2 PgC/yr to a decrease of 4.5 PgC/yr, relative to present. This additional reduction in NPP predominately occurs in the North Atlantic subtropical and subpolar gyres, as well as Atlantic eastern boundary upwelling systems. Accelerated NPP declines are the result of both surface freshening and reductions in upwelling-favorable winds enhancing phytoplankton nutrient limitation. Our findings indicate that including a dynamic Greenland ice sheet in ESMs could have large impacts on projections of future ocean circulation and biogeochemistry.

Plain Language Summary Current projections of how primary production in the oceans will respond to climate change fail to account for the impact of melting continental ice sheets. Here we use an Earth System Model (ESM) to simulate the additional impact of Greenland ice melt on 21st century primary production. The addition of Greenland meltwaters causes an acceleration of projected primary production declines in the Atlantic Ocean under a high greenhouse gas emissions scenario. Our work indicates that previous projections of declining Atlantic primary production may have underestimated reductions by not accounting for Greenland meltwaters.

Key Points:
- Projected declines in Atlantic primary production are exacerbated by simulated Greenland ice sheet melt over the 21st century
- Greenland meltwater increases phytoplankton nutrient limitation by enhancing stratification and reducing upwelling-promoting winds
- Enhanced nutrient limitation predominately suppresses primary production in Atlantic gyres and eastern boundary upwelling systems

Supporting Information:
- Supporting Information S1

Correspondence to:
L. Kwiatkowski,
lester.kwiatkowski@lmd.ens.fr

Citation:
Kwiatkowski, L., Naar, J., Bopp, L., Aumont, O., Defrance, D., & Couespel, D. (2019). Decline in Atlantic primary production accelerated by Greenland ice sheet melt. *Geophysical Research Letters*, *46*. https://doi.org/10.1029/2019GL085267

Received 3 SEP 2019
Accepted 12 OCT 2019
Accepted article online 23 OCT 2019

1. Introduction

Net primary production (NPP) in the oceans is the base of the marine food web and the primary source of energy to higher trophic levels (Chassot et al., 2010; Pauly & Christensen, 1995). NPP and the subsequent export of organic material to the deep ocean also influence atmospheric CO_2 concentrations and therefore represent an important climate feedback (Matear & Hirst, 1999). Relative changes in NPP and phytoplankton biomass are typically amplified in zooplankton (Chust et al., 2014; Stock et al., 2014), especially in the oligotrophic oceans (Kwiatkowski, Aumont, & Bopp, 2018). Accurately projecting future NPP is therefore critical to characterizing climate impacts on the marine food web and ultimately fisheries (Barange et al., 2014; Blanchard et al., 2012; Cheung et al., 2010), as well as constraining climate-carbon cycle feedbacks (Friedlingstein et al., 2006).

ESM projections of how ocean primary production will respond to future climate change have a high degree of associated uncertainty (Frölicher et al., 2016; Taucher & Oschlies, 2011). Nonetheless, across large ensembles of ESMs, there is general agreement that global ocean NPP will decline under climate change (Bopp et al., 2013; Cabré et al., 2014; Steinacher et al., 2010). Under high emissions scenarios, 21st century global NPP is projected to decline by up to 20% (Bopp et al., 2013) with declines exacerbated on multicentennial timescales (Moore et al., 2018). Such global declines are typically driven by surface ocean warming in low and midlatitudes increasingly stratifying the upper ocean and reducing nutrient concentrations in the euphotic zone of nutrient-limited waters (Bopp et al., 2013; Laufkötter et al., 2015; Steinacher et al., 2010). These declines are generally somewhat offset by shoaling of the mixed layer depth and sea ice loss reducing light limitation in high latitudes (Bopp et al., 2013; Steinacher et al., 2010).

Across ESM ensembles similar processes appear to determine the sensitivities of NPP to climate change and El Niño/Southern Oscillation climate variability. Consequently satellite observations of the sensitivity of NPP to El Niño/Southern Oscillation have been used to constrain projections of low latitude NPP decline to 3 ± 1% per degree warming in equatorial sea surface temperature (SST) (Kwiatkowski et al., 2017). Critically however, projections of future NPP, including such emergent constraints, are reliant on ESMs that do not contain coupled ice sheet models for Greenland and Antarctica.

Ice sheet meltwater has the potential to influence ocean biogeochemistry by affecting mixed layer depth and ocean circulation (Vizcaíno et al., 2008) as well as through the provision of associated nutrients (Bergeron & Tremblay, 2014; Death et al., 2014). The current absence of dynamic ice sheets in ESMs is primarily a consequence of a mismatch between the high spatial resolution required by ice sheet models and that which is computationally permissible in atmospheric and ocean components of current ESMs (Lipscomb et al., 2013). It is further complicated by difficulties in ice sheet initialization under past climatic forcing due to scarcity of observations, in addition to the community focus on century-scale climate projections, which has resulted in the inclusion of dynamic ice sheets not being prioritized. Here we use simulations of an ESM to explore the impact of idealized flash Greenland melting events on projections of 21st century primary production.

2. Materials and Methods

2.1. The ESM and Biogeochemical Model Configuration

Numerical simulations were conducted with the Institute Pierre Simon Laplace low resolution Earth System Model (IPSL-CM5A-LR; Dufresne et al., 2013) which contributed to the Coupled Model Intercomparison Project Phase 5. The ocean component has an ORCA tripolar grid with 2 ° horizontal resolution and 31 vertical levels (ORCA2; Madec, 2015) and is coupled to the Pelagic Interactions Scheme for Carbon and Ecosystem Studies (PISCES) ocean biogeochemical model (Aumont et al., 2015). PISCES describes the biogeochemical cycles of carbon and the main ocean nutrients (N, P, Fe, and Si). The model contains 24 prognostic tracers including 2 phytoplankton types (nanophytoplankton and diatoms) and 2 zooplankton size classes (microzooplankton and mesozooplankton).

In the PISCES biogeochemical model, the response of NPP to internal climate variability and long-term climate change is predominately a consequence of changes in phytoplankton growth rates (μ) (Kwiatkowski et al., 2017). In the version of the PISCES biogeochemical model that was coupled within IPSL-CM5A-LR, μ is the product of a maximum phytoplankton growth rate (μ_{max}), temperature limitation (T_f), nutrient limitation (N_{lim}), and light limitation (L_{lim}):

$$\mu = \mu_{\max} \times T_f \times N_{\lim} \times L_{\lim}, \tag{1}$$

where T_f is based on Eppley (1972),

$$T_f = e^{K_{\text{Eppley}} \times T}. \tag{2}$$

N_{lim} is defined as the most limiting nutrient limitation term for nanophytoplankton and diatoms, respectively:

$$N_{\lim}^{\text{Nano}} = \min\left(N_{PO_4}^{\text{Nano}}, N_N^{\text{Nano}}, N_{Fe}^{\text{Nano}}\right), \tag{3}$$

$$N_{\lim}^{\text{Diat}} = \min\left(N_{PO_4}^{\text{Diat}}, N_N^{\text{Diat}}, N_{Fe}^{\text{Diat}}, N_{Si}^{\text{Diat}}\right), \tag{4}$$

and L_{lim} is parameterized, based on Geider et al. (1997), as

$$L_{\lim}^{i} = f(mxl) \times \left(1 - e^{\frac{-\alpha \times \theta_{Chl}^{i} \times I_{PAR}}{\mu_{\max} \times T_f^{i} \times N_{\lim}^{i}}}\right), \tag{5}$$

where i is the phytoplankton group, α is the initial slope of the photosynthesis-irradiance curve, θ_{Chl} is the chlorophyll to carbon ratio, I_{PAR} is photosynthetically active radiation, and $f(mxl)$ represents additional limitation that occurs when the mixed layer depth exceeds the depth of the euphotic zone.

2.2. Greenland Ice Melt Simulations

The IPSL-CM5A-LR model was run under historical (1850–2005) and Representative Concentration Pathway 8.5 (RCP8.5; 2006–2100) radiative forcing, with RCP8.5 representing a business-as-usual 21st century emissions scenario (Riahi et al., 2011). Four additional freshwater hosing simulations, analogous to large and rapid Greenland ice melt, were conducted under identical 2006–2100 climate forcing. Freshwater flow of 0.05 Sv (GrIS50), 0.075 Sv (GrIS75), 0.1 Sv (GrIS100), and 0.2 Sv (GrIS200; 1 Sv = 10^6 m^3/s) was added continuously from 2006 to 2100, corresponding to additional 21st century sea level rise of approximately 43, 65, 86, and 173 cm, respectively. For context, the largest of these simulations represents the loss of approximately a quarter of the Greenland ice shelf. Model freshwater inputs were released in surface waters of regions of North Atlantic deepwater formation (45 to 65°N, 45°W to 5°E), coincident with observations of Greenland meltwater (Bamber et al., 2012; Kjeldsen et al., 2015). The idealized meltwater was assumed to lack nutrients and associated sediments. Similar simulations of freshwater hosing, conducted with the IPSL-CM5A-LR model, have previously shown that Greenland ice melt can reduce West African monsoon rainfall, increasing the vulnerability of the Sahelian agroecosystem (Defrance et al., 2017).

2.3. Assessment of NPP Drivers

Adopting present (1986–2005) and future (2090–2099) state periods, the individual drivers of changes in phytoplankton NPP were assessed by calculating temperature, light, and nutrient growth limitation terms from monthly IPSL-CM5A-LR outputs of temperature, I_{PAR}, mixed layer depth, chlorophyll, nitrate, ammonium, phosphate, silicate, and iron concentrations. All NPP and growth limitation term values are depth integrated and aggregated across phytoplankton types, unless otherwise stated. Changes in maximum monthly mixed layer depth (MLD_{max}), annual mean upwelling-favorable winds (τ_{upw}), vertical advection at 100 m, and the upward transport of NO_3 at 100 m are used to explore the mechanisms affecting NPP and phytoplankton growth limitation terms. τ_{upw} is calculated from the model output such that positive values of τ_{upw} correspond to northerly (southerly) wind stress for the Northern (Southern) Hemisphere (e.g., Rykaczewski et al., 2015). The upward vertical transport of NO_3 at 100 m is computed as the sum of fluxes that result from (1) advection, (2) diffusion, (3) isopycnal mixing, and (4) the parameterization of eddies (Gent & Mcwilliams, 1990). Although MLD_{max} is assessed across the Atlantic basin, we restrict our analysis of τ_{upw}, vertical advection, and the upward transport of NO_3 to the Canary (16–46°N, 4–29°W) and Benguela upwelling regions (8–38°S, 0–25°E).

3. Results

3.1. NPP Response to Greenland Ice Melt

The IPSL-CM5A-LR model projects global NPP declines of 3.2 PgC/yr (9%) over the 21st century under RCP8.5, with declines of 0.7 PgC/yr (17%) in the North Atlantic and 0.2 PgC/yr (4%) in the South Atlantic (Figure 1). Under the most extreme Greenland ice sheet melt scenario (GrIS200), projected global NPP declines increase by 1.3 PgC/yr over the 21st century, relative to RCP8.5. The overwhelming majority of these additional NPP reductions is confined to the Atlantic basin, with declines enhanced by 0.8 PgC/yr in the North Atlantic and 0.5 PgC/yr in the South Atlantic. The magnitude of additional NPP decline increases with the intensity of ice sheet melt scenario (Figure 1). At the end of the 21st century, there are additional NPP declines of 0.3, 0.4, and 0.9 PgC/yr for the GrIS50, GrIS75, and GrIS100 scenarios, relative to RCP8.5, respectively. Although projected NPP is influenced by climatic variability, for the majority of GrIS simulations, the suppression of NPP increases throughout the duration of simulations. However, under the most extreme scenario (GrIS200), suppression of NPP in the North Atlantic plateaus around 2060 (Figure 1).

Projected global declines in NPP are 2.0 PgC/yr (7%) for nanophytoplankton and 1.2 PgC/yr (19%) for diatoms under RCP8.5. The greater relative decline in diatom NPP is attributed to the higher nutrient half-saturation constants of diatoms and consequently their greater sensitivity to nutrient limitation (Bopp et al., 2005). Under the GrIS200 simulation, Greenland meltwater enhances the NPP declines of nanophytoplankton and diatoms by 1.1 and 0.2 PgC/yr, respectively.

The IPSL-CM5A-LR model projects RCP8.5 21st century NPP reductions that are concentrated in the North Atlantic, equatorially, and in African Eastern boundary upwelling regions (Figure 2). Greenland ice melt is projected to generally enhance the suppression of 21st century NPP under RCP8.5, across most of the

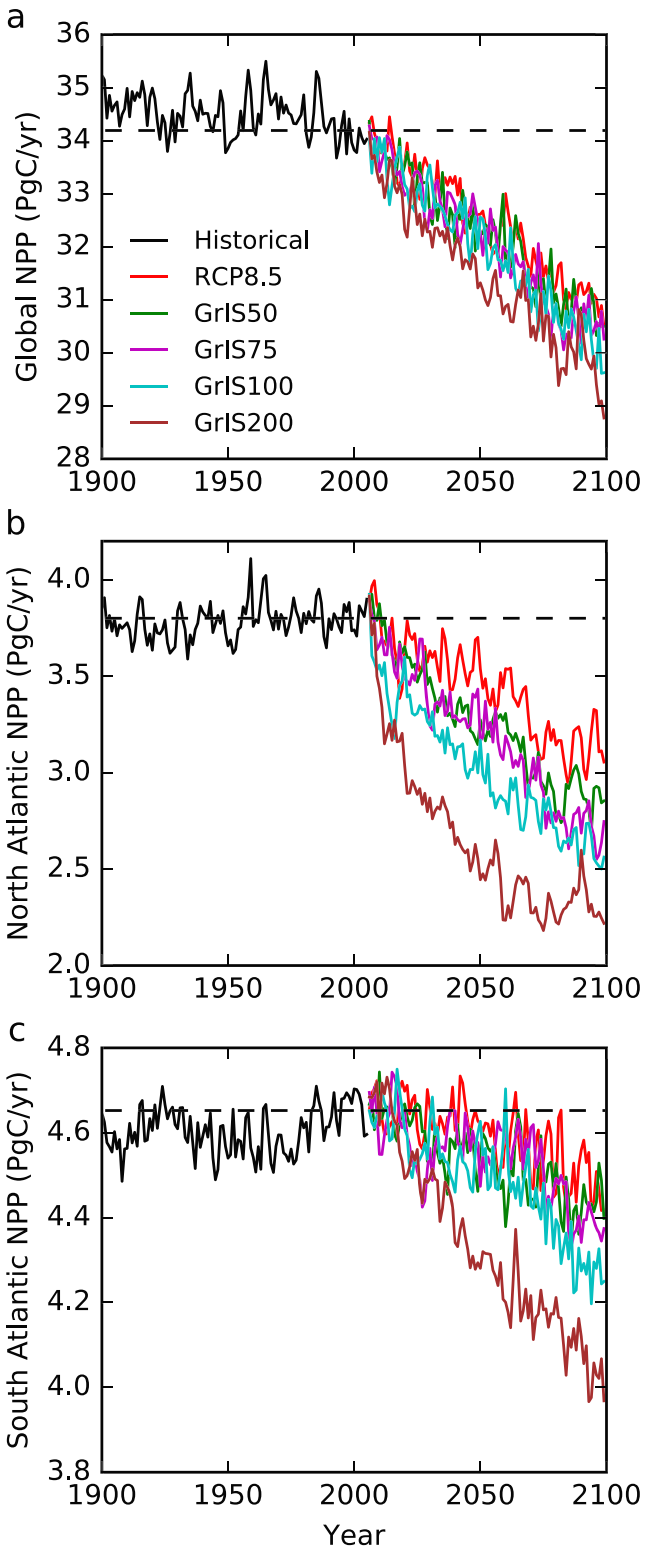

Figure 1. Projected changes in (a) global, (b) North Atlantic, and (c) South Atlantic depth integrated net primary production under the different Greenland ice melt simulations and the RCP8.5 control. Dashed black lines indicate 1986–2005 mean historical values.

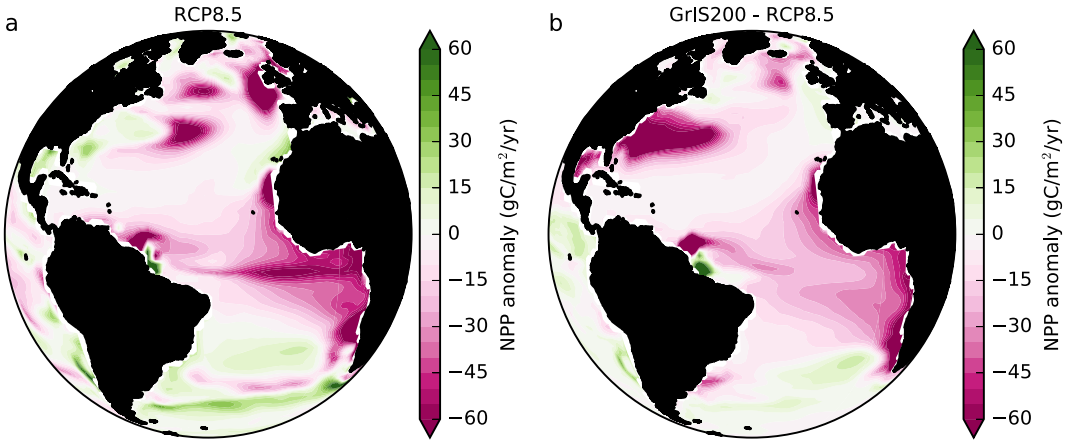

Figure 2. (a) Twenty-first century (2090–2099) NPP anomalies under RCP8.5 relative to historical (1986–2005) simulations. (b) End of century (2090–2099) NPP anomalies between the GrIS200 simulation and the RCP8.5 control.

Atlantic basin. However, the greatest enhancements of NPP suppression occur in the North Atlantic subtropical gyre and African Eastern boundary upwelling regions, where NPP under GrIS200 can be reduced by 30–70 $gC \cdot m^{-2} \cdot yr^{-1}$ relative to RCP8.5 (Figure 2).

In the first 15 years of the GrIS simulations, the enhanced suppression of NPP predominately occurs near Greenland and in the North Atlantic subpolar gyre, while there is a small region of NPP increase in the Canary Current System (Figure S1). From 2020 onward, enhanced suppression of NPP increasingly occurs in the North Atlantic subtropical gyre and the Atlantic eastern boundary upwelling regions of both the Northern and Southern Hemispheres (Figure S1). The Canary Current region that initially experiences enhanced NPP increasingly exhibits NPP suppression, while small regions of NPP suppression and enhancement are present near the Amazon estuary. This temporal progression and spatial pattern of enhanced NPP declines relative to RCP8.5 are consistent across the four GrIS simulations (Figure S2).

3.2. Phytoplankton Growth Rate Limitation

Given that L_{lim} in the PISCES model is not independent of other phytoplankton growth rate limitation terms (equation (5)), we confine our analysis here to the impact on T_f and N_{lim}. Further analysis of the response of L_{lim} is provided in the supporting material. The influence of Greenland meltwaters on nanophytoplankton T_f and N_{lim} is shown in Figure 3. T_f and N_{lim} are depth integrated and weighted by the vertical concentration of mean historical (1986–2005) nanophytoplankton biomass. As such, the T_f and N_{lim} anomalies reflect changes in growth limitation terms that impact the vertically integrated NPP of each grid cell. Greenland ice melt is shown to have limited impact on the temperature limitation of nanophytoplankton growth rates. In the North Atlantic subpolar gyre, T_f increases slightly (<15%) representing temperature increases that act to enhance phytoplankton growth rates, whereas in the rest of the North Atlantic, T_f declines slightly (<15%). In the Southern Hemisphere, T_f generally exhibits increases of a similar order of magnitude.

The impact of Greenland ice melt on nanophytoplankton nutrient limitation is considerably greater than its impact on temperature limitation. N_{lim} decreases substantially (>30%) in the North Atlantic subtropical gyre and the Atlantic eastern boundary upwelling regions of the Northern and Southern Hemispheres. This represents an increase in nutrient limitation that acts to suppress nanophytoplankton growth rates in these regions (Figure 3b). In contrast with changes in temperature limitation, the regions of greater nutrient limitation are strongly coincident with the areas of enhanced NPP decline. As such, the dominant driver of enhanced NPP reductions in the GrIS simulations is greater nutrient limitation, with minor additional influence due to changes in temperature and light limitation (Figure S3). The spatial pattern of anomalies in diatom growth limitation terms is broadly similar to that of nanophytoplankton (Figure S4). The magnitude of anomalies differs however, due to the growth parameterization and biomass distribution of each plankton functional type.

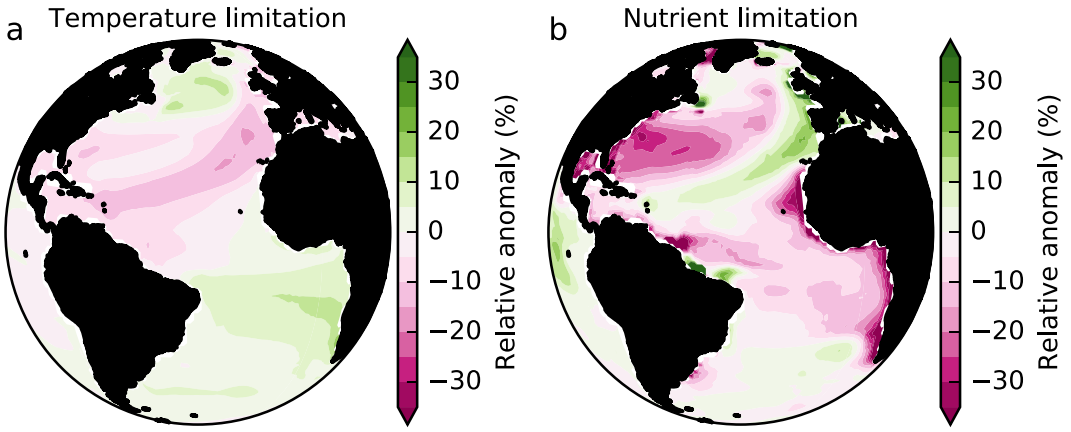

Figure 3. End of the 21st century (2090–2099) nanophytoplankton temperature (T_f) and nutrient (N_{lim}) limitation anomalies between the GrIS200 simulation and the RCP8.5 control. Growth rate limitation terms are depth integrated and weighted by the vertical concentration of historical nanophytoplankton biomass. Negative values indicate an increase in limitation (i.e., lower temperatures or nutrient concentrations), which acts to suppress nanophytoplankton growth rates in the GrIS200 scenario relative to RCP8.5.

3.3. Stratification and Upwelling Intensity

The reduction in phytoplankton growth rates and therefore NPP, in response to enhanced nutrient limitation in the GrIS simulations, can be attributed to changes in both stratification and the intensity of eastern boundary upwelling. The impact of increased stratification, as a consequence of surface freshening, is evident in shoaling of MLD_{max}. The MLD_{max} in the GrIS200 simulation shoals by up to 20 m, relative to RCP8.5, in the North Atlantic subpolar and subtropical gyres by the end of the 21st century (Figure 4a). This results in less nutrient-rich deep waters being mixed into the euphotic zone and, in areas of typically high nutrient limitation such as the subtropical gyre, explains the enhanced NPP declines.

The enhanced nutrient limitation and subsequent declines in NPP that occur in the Atlantic eastern boundary upwelling systems are the result of changes in both stratification and upwelling. In the Benguela Current region, there is strong coherence between declines in upwelling-favorable winds (τ_{upw}) and declines in the vertical supply of NO_3 in the GrIS200 simulation (Figure 4). The reduction in NO_3 supply, which enhances nutrient limitation and drives the observed declines in NPP in this region, can be explained by reduced vertical advection (upwelling), alongside reductions in the vertical mixing of nutrients into the upper ocean. In the Canary Current region, τ_{upw} generally increases in the GrIS200 simulation relative to RCP8.5 (Figure 4b), with vertical advection predominately increasing (Figure 4d). However, south of the Canary Islands the vertical supply of NO_3, which is driven by both advection and mixing, declines. This is the location of greater nutrient limitation and declining NPP. North of the Canary Islands, the vertical supply of NO_3 shows limited increases, and there is reduced nutrient limitation; however coincident increases in temperature limitation offset any potential impact on NPP.

4. Discussion

4.1. Mechanisms of Enhanced NPP Decline Under Greenland Ice Melt

It is somewhat expected that the simulation of Greenland ice melt results in enhanced regional declines in NPP. Greater phytoplankton nutrient limitation, in response to surface warming that intensifies stratification, is typically the dominant driver of projected 21st century NPP declines, across ESMs (Bopp et al., 2013; Steinacher et al., 2010). Our simulations of Greenland ice melt freshen local surface and upper ocean waters, thereby increasing the gradient of vertical density profiles and further enhancing thermally driven increases in stratification. This shoals the MLD_{max} and reduces the mixing of nutrient-rich deep waters into the upper ocean.

It is, however, slightly counterintuitive that such a large proportion (38%) of enhanced Atlantic basin NPP declines occur in the Southern Hemisphere and in particular in the eastern boundary upwelling regions.

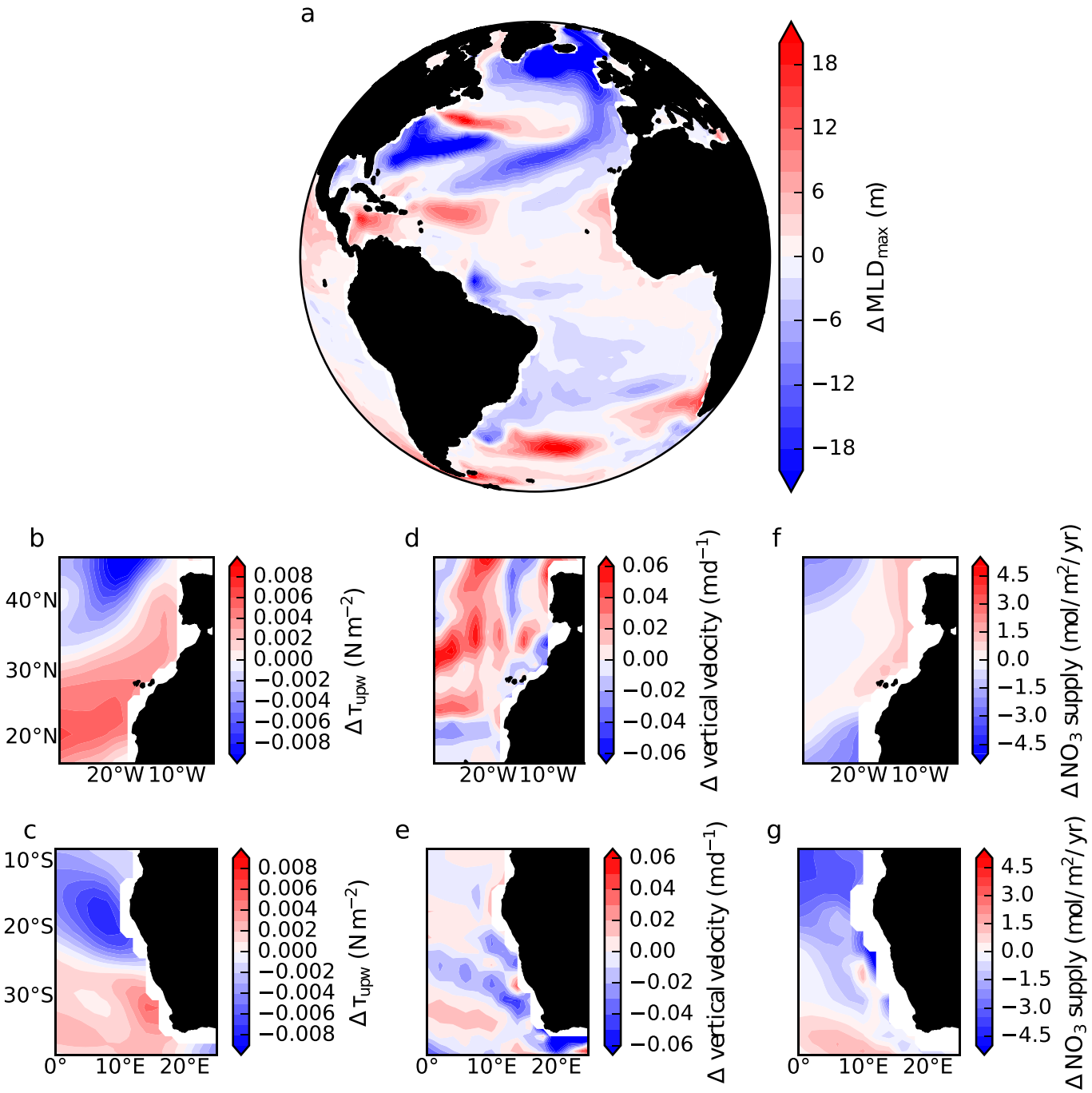

Figure 4. Impact of Greenland ice melt on mixed layer depth, upwelling-favorable winds, vertical advection, and nutrient supply. End of the 21st century (2090–2099) anomalies between GrIS200 and RCP8.5 simulations of (a) maximum mixed layer depth (MLD_{max}), (b–c) upwelling-favorable winds (τ_{upw}), (d–e) vertical advection velocities at 100 m, and (f–g) vertical transport of NO_3 at 100 m. Positive values indicate that Greenland ice melt results in a relative increase in MLD_{max}, τ_{upw}, upward vertical advection, and upward NO_3 transport.

These enhanced NPP declines are related to atmospheric teleconnections and ocean-atmosphere coupling. As shown by Defrance et al. (2017), similar simulations of Greenland ice melt in the same IPSL-CM5A-LR model result in a slowdown of the Atlantic meridional overturning circulation and negative Northern Hemisphere surface temperature anomalies. Positive sea level pressure anomalies develop over the Sahel, while negative anomalies develop in the Gulf of Guinea. This pressure gradient produces low-level wind

anomalies, which reduce rainfall associated with the West African monsoon. Here we show that Greenland ice melt also acts to reduce τ_{upw} in the Benguela Current region, decreasing the vertical supply of nutrient-rich deep waters and in turn reducing NPP both in the coastal region and more generally across the South Atlantic. The reduction in τ_{upw} in the Benguela Current region is due to the development of low-level positive temperature anomalies over the South Atlantic and negative temperature anomalies over the adjacent African continental landmass (Figure S5). This acts to reduce land-ocean sea level pressure gradients and consequently decrease upwelling-favorable winds.

It should be noted that climate change has often been hypothesized to intensify eastern boundary upwelling, due to greater continental warming and intensification of land-ocean atmospheric pressure gradients (Bakun, 1990). Recent ESMs, however, generally project an equatorward reduction in τ_{upw} and poleward intensification of τ_{upw} associated with the poleward extension of high-pressure atmospheric cells (Rykaczewski et al., 2015). In the RCP8.5 simulation, the IPSL-CM5A-LR model exhibits a similar poleward displacement of τ_{upw} in the Atlantic (Figure S6). However, the additional simulation of Greenland ice melt modifies this, particularly in the Southern Hemisphere where the poleward displacement of τ_{upw} is intensified (Figure 4).

4.2. Caveats and Limitations

The Greenland ice sheet meltwater simulations presented herein are, by design, highly idealized. The ocean circulation response in IPSL-CM5A-LR is likely to differ in higher resolution models that resolve Greenland boundary currents, which might otherwise divert meltwaters away from deep convection regions (Weijer et al., 2012). Interactions with Antarctic Ice Sheet loss, which has been projected to enhance Southern Ocean primary production (Death et al., 2014; Person et al., 2019), are not explored. Moreover, the magnitude of simulated freshwater discharge is notably high compared to both recent observations of the Greenland contribution to global sea level rise (0.77 mm/yr; Bamber et al., 2018) and process-based estimates of the contribution to sea level rise under RCP8.5 (6–33 cm in 2100; Vizcaino et al., 2015; Fürst et al., 2015; Aschwanden et al., 2019). The duration of simulations is also relatively short compared to the likely multi-centennial timescales of future ice loss. Given limited resources, our approach maximizes signal-to-noise ratios and reveals ocean-climate dynamics that might not be apparent under lesser freshwater forcing, without computationally prohibitive large-ensemble or long-duration simulations. Nonetheless, although unlikely, even the most extreme meltwater simulation is arguably plausible given paleorecords of meltwater pulse events that resulted in >40 $mm \cdot yr^{-1}$ sea level rise (Deschamps et al., 2012).

In addition, given the uncertainty associated with ESM ensemble NPP projections (Bopp et al., 2013), the impact of Greenland ice melt on projected NPP is likely to exhibit some degree of ESM dependence. Indeed, diverse ocean biogeochemical models coupled to the same physical ocean model can project a wide variety of NPP responses to identical physical ocean forcing (Kwiatkowski et al., 2014). As such, our results should be validated with alternative ESM and ocean biogeochemical model configurations.

4.2.1. Glacial Nutrients and Subglacial Discharge

Perhaps the greatest limitation of our model results is that we assume freshwater fluxes do not contain nutrients. There is emerging evidence that Greenland meltwater is a potential source of bioavailable iron (Bhatia et al., 2013; Hawkings et al., 2014) and N-rich dissolved organic matter (Lawson et al., 2014) to the North Atlantic. Furthermore, models of subglacial Greenland discharge have shown that the depth of glacier grounding lines can result in the entrainment of limiting nutrients into discharge plumes (Cape et al., 2019; Hopwood et al., 2018). Our idealized surface hosing simulations do not capture interactions between grounding line depth, subsurface discharge, and plume nutrient entrainment, which are likely to influence projections of localized primary production. Although we currently lack the data to constrain estimates of these nutrient fluxes, they could potentially compensate for stratification-driven reductions in euphotic zone nutrients. Indeed, simulations of Antarctic Ice Sheet meltwaters rich in iron have shown enhanced NPP in the Southern Ocean (Death et al., 2014; Person et al., 2019). The importance of iron for NPP in the North Atlantic is considerably less than in the Southern Ocean however, where iron is the main limiting nutrient. As such, the extent of Southern Ocean iron fertilization seen in model simulations is unlikely to be replicated in the North Atlantic with comparable Greenland simulations. Moreover, a fertilization effect due to Greenland meltwaters is likely to be highest locally and has limited impact on projected NPP declines in the subtropical gyre. It should almost certainly not influence the NPP declines in upwelling regions,

which are driven by ocean-atmosphere teleconnections. Nonetheless, further sensitivity studies should be conducted to assess the aggregate impacts on basin-scale NPP.

4.2.2. Phytoplankton Stoichiometry

A further caveat of this study is the use of an ocean biogeochemical model (PISCES) with fixed C:N:P phytoplankton stoichiometry. Such Monod formulations are computationally efficient and therefore used as standard in ESMs, despite observations that phytoplankton exhibits varying degrees of stoichiometric plasticity (Moreno & Martiny, 2018). NPP projections in ocean biogeochemical models that incorporate variable C:N:P phytoplankton stoichiometry can be less sensitive to enhanced nutrient limitation under climate change (Kwiatkowski, Aumont, Bopp, & Ciais, 2018), while reductions in zooplankton growth efficiency can enhance trophic amplification of biomass declines in such models (Kwiatkowski, Aumont, & Bopp, 2018). Future work should assess the extent to which variable phytoplankton stoichiometry may moderate the impact of Greenland ice melt on primary production.

5. Conclusions

Using a coupled ESM, this study explores the potential impact of rapid Greenland ice sheet melt on 21st century projections of NPP, under a business-as-usual emissions scenario. The simulation of surface ocean freshening, in Atlantic waters of Greenland meltwater discharge, results in additional suppression of projected 21st century NPP. This enhanced NPP suppression predominately occurs in the North Atlantic subtropical and subpolar gyres, as well as Atlantic eastern boundary upwelling systems, and is shown to be largely due to greater phytoplankton nutrient limitation. Projected increases in phytoplankton nutrient limitation are the result of both enhanced stratification in the North Atlantic and atmospheric teleconnections that reduce upwelling-favorable winds, particularly in the Benguela Current region. Although highly idealized, our simulations indicate that dynamic ice sheets could have dramatic impacts on projections of ocean circulation and biogeochemistry. As such, their incorporation in ESMs should be considered a future priority.

Acknowledgments
This study has received funding from the European Union's Horizon 2020 research and innovation program under grant agreement 641816 (CRESCENDO) and the Agence Nationale de la Recherche grant agreement ANR-17-CE32-0008 (CIGOEF) and ANR-18-ERC2-0001-01 (CONVINCE). The study benefited from the high performance computing (HPC) resources made available by Grand Equipement National de Calcul Intensif, CEA, and Centre National de la Recherche Scientifique. It also benefited from the IPSL Prodiguer-Ciclad facility, which is supported by CNRS, UPMC, and Labex L-IPSL and is funded by the ANR (ref ANR-10-LABX-0018) and the European FP7 IS-ENES2 project (ref 312979). The authors declare no conflict of interests. The IPSL-CM5A-LR model output data is available on Zonedo (doi: 10.5281/zenodo.3384914).

References

Aschwanden, A., Fahnestock, M. A., Truffer, M., Brinkerhoff, D. J., Hock, R., Khroulev, C., et al. (2019). Contribution of the Greenland ice sheet to sea level over the next millennium. *Science Advances*, *5*(6), eaav9396. https://doi.org/10.1126/sciadv.aav9396

Aumont, O., Ethé, C., Tagliabue, A., Bopp, L., & Gehlen, M. (2015). PISCES-v2: An ocean biogeochemical model for carbon and ecosystem studies. *Geoscientific Model Development*, *8*(8), 2465–2513. https://doi.org/10.5194/gmd-8-2465-2015

Bakun, A. (1990). Global climate change and intensification of coastal ocean upwelling. *Science*, *247*(4939), 198–201. https://doi.org/10.1126/science.247.4939.198

Bamber, J., van den Broeke, M., Ettema, J., Lenaerts, J., & Rignot, E. (2012). Recent large increases in freshwater fluxes from Greenland into the North Atlantic. *Geophysical Research Letters*, *39*, L19501. https://doi.org/10.1029/2012GL052552

Bamber, J. L., Westaway, R. M., Marzeion, B., & Wouters, B. (2018). The land ice contribution to sea level during the satellite era. *Environmental Research Letters*, *13*(6). https://doi.org/10.1088/1748-9326/aac2f0

Barange, M., Merino, G., Blanchard, J. L., Scholtens, J., Harle, J., Allison, E. H., et al. (2014). Impacts of climate change on marine ecosystem production in societies dependent on fisheries. *Nature Climate Change*, *4*(3), 211–216. https://doi.org/10.1038/nclimate2119

Bergeron, M., & Tremblay, J.-É. (2014). Shifts in biological productivity inferred from nutrient drawdown in the southern Beaufort Sea (2003–2011) and northern Baffin Bay (1997–2011), Canadian Arctic. *Geophysical Research Letters*, *41*, 3979–3987. https://doi.org/10.1002/2014GL059649

Bhatia, M. P., Kujawinski, E. B., Das, S. B., Breier, C. F., Henderson, P. B., & Charette, M. A. (2013). Greenland meltwater as a significant and potentially bioavailable source of iron to the ocean. *Nature Geoscience*, *6*(4), 274–278. https://doi.org/10.1038/ngeo1746

Blanchard, J. L., Jennings, S., Holmes, R., Harle, J., Merino, G., Allen, J. I., et al. (2012). Potential consequences of climate change for primary production and fish production in large marine ecosystems. *Philosophical Transactions of the Royal Society B*, *367*(1605), 2979–2989. https://doi.org/10.1098/rstb.2012.0231

Bopp, L., Aumont, O., Cadule, P., Alvain, S., & Gehlen, M. (2005). Response of diatoms distribution to global warming and potential implications: A global model study. *Geophysical Research Letters*, *32*, L19606. https://doi.org/10.1029/2005GL023653

Bopp, L., Resplandy, L., Orr, J. C., Doney, S. C., Dunne, J. P., Gehlen, M., et al. (2013). Multiple stressors of ocean ecosystems in the 21st century: Projections with CMIP5 models. *Biogeosciences*, *10*(10), 6225–6245. https://doi.org/10.5194/bg-10-6225-2013

Cabré, A., Marinov, I., & Leung, S. (2014). Consistent global responses of marine ecosystems to future climate change across the IPCC AR5 earth system models. *Climate Dynamics*, *45*(5–6), 1253–1280. https://doi.org/10.1007/s00382-014-2374-3

Cape, M. R., Straneo, F., Beaird, N., Bundy, R. M., & Charette, M. A. (2019). Nutrient release to oceans from buoyancy-driven upwelling at Greenland tidewater glaciers. *Nature Geoscience*, *12*(1), 34. https://doi.org/10.1038/s41561-018-0268-4

Chassot, E., Bonhommeau, S., Dulvy, N. K., Mélin, F., Watson, R., Gascuel, D., & Le Pape, O. (2010). Global marine primary production constrains fisheries catches. *Ecology Letters*, *13*(4), 495–505. https://doi.org/10.1111/j.1461-0248.2010.01443.x

Cheung, W. W. L., Lam, V. W. Y., Sarmiento, J. L., Kearney, K., Watson, R., Zeller, D., & Pauly, D. (2010). Large-scale redistribution of maximum fisheries catch potential in the global ocean under climate change. *Global Change Biology*, *16*(1), 24–35. https://doi.org/10.1111/j.1365-2486.2009.01995.x

Chust, G., Allen, J. I., Bopp, L., Schrum, C., Holt, J., Tsiaras, K., et al. (2014). Biomass changes and trophic amplification of plankton in a warmer ocean. *Global Change Biology*, *20*(7), 2124–2139. https://doi.org/10.1111/gcb.12562

Death, R., Wadham, J. L., Monteiro, F., le Brocq, A. M., Tranter, M., Ridgwell, A., et al. (2014). Antarctic Ice Sheet fertilises the Southern Ocean. *Biogeosciences*, *11*(10), 2635–2643. https://doi.org/10.5194/bg-11-2635-2014

Defrance, D., Ramstein, G., Charbit, S., Vrac, M., Famien, A. M., Sultan, B., et al. (2017). Consequences of rapid ice sheet melting on the Sahelian population vulnerability. *Proceedings of the National Academy of Sciences*, *114*(25), 6533–6538. https://doi.org/10.1073/pnas.1619358114

Deschamps, P., Durand, N., Bard, E., Hamelin, B., Camoin, G., Thomas, A. L., et al. (2012). Ice-sheet collapse and sea-level rise at the Bølling warming 14,600 years ago. *Nature*, *483*(7391), 559–564. https://doi.org/10.1038/nature10902

Dufresne, J.-L., Foujols, M. A., Denvil, S., Caubel, A., Marti, O., Aumont, O., et al. (2013). Climate change projections using the IPSL-CM5 Earth System Model: from CMIP3 to CMIP5. *Climate Dynamics*, *40*(9–10), 2123–2165. https://doi.org/10.1007/s00382-012-1636-1

Eppley, R. W. (1972). Temperature and phytoplankton growth in the sea. *Fishery Bulletin*, *70*, 1063–1085.

Friedlingstein, P., Cox, P., Betts, R., Bopp, L., von Bloh, W., Brovkin, V., et al. (2006). Climate–carbon cycle feedback analysis: results from the C4MIP model intercomparison. *Journal of Climate*, *19*(14), 3337–3353. https://doi.org/10.1175/JCLI3800.1

Frölicher, T. L., Rodgers, K. B., Stock, C. A., & Cheung, W. W. L. (2016). Sources of uncertainties in 21st century projections of potential ocean ecosystem stressors. *Global Biogeochemical Cycles*, *30*, 1224–1243. https://doi.org/10.1002/2015GB005338

Fürst, J. J., Goelzer, H., & Huybrechts, P. (2015). Ice-dynamic projections of the Greenland ice sheet in response to atmospheric and oceanic warming. *The Cryosphere*, *9*(3), 1039–1062. https://doi.org/10.5194/tc-9-1039-2015

Geider, R., MacIntyre, H., & Kana, T. (1997). Dynamic model of phytoplankton growth and acclimation: Responses of the balanced growth rate and the chlorophyll a: Carbon ratio to light, nutrient-limitation and temperature. *Marine Ecology Progress Series*, *148*, 187–200. https://doi.org/10.3354/meps148187

Gent, P. R., & Mcwilliams, J. C. (1990). Isopycnal mixing in ocean circulation models. *Journal of Physical Oceanography*, *20*(1), 150–155. https://doi.org/10.1175/1520-0485(1990)020<0150:IMIOCM>2.0.CO;2

Hawkings, J. R., Wadham, J. L., Tranter, M., Raiswell, R., Benning, L. G., Statham, P. J., et al. (2014). Ice sheets as a significant source of highly reactive nanoparticulate iron to the oceans. *Nature Communications*, *5*(1), 3929. https://doi.org/10.1038/ncomms4929

Hopwood, M. J., Carroll, D., Browning, T. J., Meire, L., Mortensen, J., Krisch, S., & Achterberg, E. P. (2018). Non-linear response of summertime marine productivity to increased meltwater discharge around Greenland. *Nature Communications*, *9*(1), 3256. https://doi.org/10.1038/s41467-018-05488-8

Kjeldsen, K. K., Korsgaard, N. J., Bjørk, A. A., Khan, S. A., Box, J. E., Funder, S., et al. (2015). Spatial and temporal distribution of mass loss from the Greenland ice sheet since AD 1900. *Nature*, *528*(7582), 396–400. https://doi.org/10.1038/nature16183

Kwiatkowski, L., Aumont, O., & Bopp, L. (2018). Consistent trophic amplification of marine biomass declines under climate change. *Global Change Biology*, *25*(1), 218–229. https://doi.org/10.1111/gcb.14468

Kwiatkowski, L., Aumont, O., Bopp, L., & Ciais, P. (2018). The impact of variable phytoplankton stoichiometry on projections of primary production, food quality, and carbon uptake in the global ocean. *Global Biogeochemical Cycles*, *32*, 516–528. https://doi.org/10.1002/2017GB005799

Kwiatkowski, L., Bopp, L., Aumont, O., Ciais, P., Cox, P. M., Laufkötter, C., et al. (2017). Emergent constraints on projections of declining primary production in the tropical oceans. *Nature Climate Change*, *7*(5), 355–358. https://doi.org/10.1038/nclimate3265

Kwiatkowski, L., Yool, A., Allen, J. I., Anderson, T. R., Barciela, R., Buitenhuis, E. T., et al. (2014). iMarNet: An ocean biogeochemistry model intercomparison project within a common physical ocean modelling framework. *Biogeosciences*, *11*(24), 7291–7304. https://doi.org/10.5194/bg-11-7291-2014

Laufkötter, C., Vogt, M., Gruber, N., Aita-Noguchi, M., Aumont, O., Bopp, L., et al. (2015). Drivers and uncertainties of future global marine primary production in marine ecosystem models. *Biogeosciences*, *12*(23), 6955–6984. https://doi.org/10.5194/bg-12-6955-2015

Lawson, E. C., Bhatia, M. P., Wadham, J. L., & Kujawinski, E. B. (2014). Continuous summer export of nitrogen-rich organic matter from the Greenland ice sheet inferred by ultrahigh resolution mass spectrometry. *Environmental Science & Technology*, *48*(24), 14,248–14,257. https://doi.org/10.1021/es501732h

Lipscomb, W. H., Fyke, J. G., Vizcaíno, M., Sacks, W. J., Wolfe, J., Vertenstein, M., et al. (2013). Implementation and initial evaluation of the Glimmer Community ice sheet model in the Community Earth System Model. *Journal of Climate*, *26*(19), 7352–7371. https://doi.org/10.1175/JCLI-D-12-00557.1

Madec, G. (2015). *NEMO ocean engine*. France: Institut Pierre-Simon Laplace (IPSL).

Matear, R. J., & Hirst, A. C. (1999). Climate change feedback on the future oceanic CO_2 uptake. *Tellus Series B: Chemical and Physical Meteorology*, *51*(3), 722–733. https://doi.org/10.3402/tellusb.v51i3.16472

Moore, J. K., Fu, W., Primeau, F., Britten, G. L., Lindsay, K., Long, M., et al. (2018). Sustained climate warming drives declining marine biological productivity. *Science*, *359*(6380), 1139–1143. https://doi.org/10.1126/science.aao6379

Moreno, A. R., & Martiny, A. C. (2018). Ecological stoichiometry of ocean plankton. *Annual Review of Marine Science*, *10*(1), 43–69. https://doi.org/10.1146/annurev-marine-121916-063126

Pauly, D., & Christensen, V. (1995). Primary production required to sustain global fisheries. *Nature*, *374*, 255–257. https://doi.org/10.1038/374255a0

Person, R., Aumont, O., Madec, G., Vancoppenolle, M., Bopp, L., & Merino, N. (2019). Sensitivity of ocean biogeochemistry to the iron supply from the Antarctic Ice Sheet explored with a biogeochemical model. *Biogeosciences*, *16*(18), 3583–3603. https://doi.org/10.5194/bg-16-3583-2019

Riahi, K., Rao, S., Krey, V., Cho, C., Chirkov, V., Fischer, G., et al. (2011). RCP 8.5—A scenario of comparatively high greenhouse gas emissions. *Climatic Change*, *109*(1–2), 33–57. https://doi.org/10.1007/s10584-011-0149-y

Rykaczewski, R. R., Dunne, J. P., Sydeman, W. J., García-Reyes, M., Black, B. A., & Bograd, S. J. (2015). Poleward displacement of coastal upwelling-favorable winds in the ocean's eastern boundary currents through the 21st century. *Geophysical Research Letters*, *42*, 6424–6431. https://doi.org/10.1002/2015GL064694

Steinacher, M., Joos, F., Frölicher, T. L., Bopp, L., Cadule, P., Cocco, V., et al. (2010). Projected 21st century decrease in marine productivity: A multi-model analysis. *Biogeosciences*, *7*(3), 979–1005. https://doi.org/10.5194/bg-7-979-2010

Stock, C. A., Dunne, J. P., & John, J. G. (2014). Drivers of trophic amplification of ocean productivity trends in a changing climate. *Biogeosciences*, *11*(24), 7125–7135. https://doi.org/10.5194/bg-11-7125-2014

Taucher, J., & Oschlies, A. (2011). Can we predict the direction of marine primary production change under global warming? *Geophysical Research Letters*, *38*, L02603. https://doi.org/10.1029/2010GL045934

Vizcaíno, M., Mikolajewicz, U., Gröger, M., Maier-Reimer, E., Schurgers, G., & Winguth, A. M. E. (2008). Long-term ice sheet–climate interactions under anthropogenic greenhouse forcing simulated with a complex Earth System Model. *Climate Dynamics*, *31*(6), 665–690. https://doi.org/10.1007/s00382-008-0369-7

Vizcaino, M., Mikolajewicz, U., Ziemen, F., Rodehacke, C. B., Greve, R., & Broeke, M. R. (2015). Coupled simulations of Greenland ice sheet and climate change up to A.D. 2300. *Geophysical Research Letters*, *42*, 3927–3935. https://doi.org/10.1002/2014GL061142

Weijer, W., Maltrud, M. E., Hecht, M. W., Dijkstra, H. A., & Kliphuis, M. A. (2012). Response of the Atlantic Ocean circulation to Greenland ice sheet melting in a strongly-eddying ocean model. *Geophysical Research Letters*, *39*, L09606. https://doi.org/10.1029/2012GL051611